

# SCN5A Rare Variants in Familial Dilated Cardiomyopathy Decrease Peak Sodium Current Depending on the Common Polymorphism H558R and Common Splice Variant Q1077del

Jianding Cheng, M.D., Ph.D.<sup>1,2</sup>, Ana Morales, M.S., C.G.C.<sup>3</sup>, Jill D. Siegfried, M.S., C.G.C.<sup>3</sup>, Duanxiang Li, M.D., M.S.<sup>3</sup>, Nadine Norton, Ph.D.<sup>3</sup>, Junyao Song<sup>1</sup>, Jorge Gonzalez-Quintana, B.S.<sup>3</sup>, Jonathan C. Makielski, M.D.<sup>1</sup>, and Ray E. Hershberger, M.D.<sup>3</sup>

## Abstract

Obtaining functional data with newly identified rare variants increases certainty that the variant identified is relevant for dilated cardiomyopathy (DCM) causation. Two novel *SCN5A* rare variants, R222Q and I1835T, segregated with DCM in two families with affected individuals homozygous or heterozygous for the common *SCN5A* polymorphism H558R. cDNAs with each rare variant were constructed in the common Q1077del or Q1077 splice variant backgrounds with and without the H558R polymorphism and expressed in HEK293 cells. Sodium current ( $I_{Na}$ ) was studied for each using whole-cell voltage clamp. In the Q1077del background  $I_{Na}$  densities of R222Q and I1835T were not different from wild type, but the combined variants of R222Q/H558R, I1835T/H558R caused approximately 35% and approximately 30% reduction, respectively, and each showed slower recovery from inactivation. In the Q1077del background R222Q and R222Q/H558R also exhibited a significant negative shift in both activation and inactivation while I1835T/H558R showed a significant negative shift in inactivation that tended to decrease window current. In contrast, expression in the Q1077 background showed no changes in peak  $I_{Na}$  densities, decay, or recovery from inactivation for R222Q/H558R and I1835T/H558R. We conclude that the biophysical findings, dependent upon common *SCN5A* variants, provide further evidence that these novel *SCN5A* rare variants are relevant for DCM. Clin Trans Sci 2010; Volume 3: 287–294

**Keywords:** dilated cardiomyopathy, ion channels, sodium current, polymorphism, splice variants

## Introduction

The genetic causes of dilated cardiomyopathy (DCM), the most common form of cardiomyopathy and the primary indication for heart transplantation, have been linked to mutations in over 30 genes.<sup>1</sup> These genes encode proteins of the cytoskeleton and contractile apparatus, the nuclear membrane protein lamin A/C, the regulatory subunit of the  $K_{ATP}$  channel,  $Ca^{2+}$ -handling proteins and others.<sup>1</sup> In recent years, mutations in the *SCN5A*-encoded pore-forming  $\alpha$  subunit of the cardiac sodium channel ( $Na_v1.5$ ) have been implicated to cause DCM.<sup>2–6</sup> So far, most DCM cases with *SCN5A* mutations have also had conduction system disease (CSD), suggesting that loss of function of  $Na_v1.5$  may be related to the development of DCM.<sup>7</sup>

However, the functional characterization of DCM-related *SCN5A* mutations has so far revealed diverse biophysical properties. The DCM-associated mutations W156X,<sup>2</sup> T220I,<sup>8</sup> R225W,<sup>2</sup> R814Q,<sup>9</sup> and D1595N<sup>10</sup> caused varying degrees of  $I_{Na}$  density from complete ablation to mild reduction, while D1275N<sup>11</sup> and D1595H<sup>6</sup> showed unaffected peak  $I_{Na}$  densities. Although R814W<sup>6</sup> and a more recently reported A1180V<sup>5</sup> tended to reduce  $I_{Na}$  at high frequencies, R814W<sup>6</sup> also displayed increased window current and A1180V<sup>5</sup> caused a gain of function of increased late  $I_{Na}$ . In addition, the gating kinetics in these mutations with unchanged peak  $I_{Na}$  densities did not necessarily result in decreased  $I_{Na}$ .

We identified two novel *SCN5A* mutations (R222Q and I1835T) in probands with familial DCM (FDC)<sup>12</sup> and sought functional data to increase the certainty that these rare variants were relevant for disease. Interestingly, both of the probands carried the H558R polymorphism that is present in approximately 20% of individuals.<sup>13</sup> We have previously shown that the H558R polymorphism along with the alternative splice variants (Q1077del and Q1077) interact with *SCN5A* mutations to cause variable biophysical phenotypes.<sup>13–15</sup> The present study

investigated the clinical, molecular genetic, and biophysical phenotypes of these two mutations combined with H558R in both splice variant backgrounds. We show that the DCM-related *SCN5A* rare variants perturb the *SCN5A* biophysical phenotype that is modulated by *SCN5A* common variants. Collectively, these data strengthen the evidence that the identified rare variants are relevant for DCM causation.

## Materials and Methods

### Patient population

Written, informed consent was obtained from probands and available family members. A blood sample was obtained for genetic research. Medical family history was obtained and a pedigree was constructed. Idiopathic DCM (IDC) was defined as left ventricular (LV) enlargement with systolic dysfunction (ejection fraction [EF] <50%) and coronary artery disease, cardiotoxic exposure and other known causes ruled out.<sup>16</sup> The study was approved by the Oregon Health & Science University and the University of Miami Institutional Review Boards.

### Genetic analysis

Genomic DNA was extracted from whole blood. All exons and intron/exon boundaries were polymerase chain reaction (PCR) amplified by standard methods in our laboratory<sup>17,18</sup> or at Seattle SNPs under contract to the NHLBI resequencing service.<sup>12</sup> Samples from probands who carried *SCN5A* protein-altering variants, as well as any available samples from their relatives, were resequenced in our laboratory for confirmation and segregation analysis. Testing for H558R was also conducted in our laboratory.

<sup>1</sup>Division of Cardiovascular Medicine, Department of Medicine, University of Wisconsin, Madison, Wisconsin, USA; <sup>2</sup>Department of Forensic Pathology, Zhongshan School of Medicine, Sun Yat-sen University, Guangzhou, Guangdong, China; <sup>3</sup>Cardiovascular Division, University of Miami Miller School of Medicine, Miami, Florida, USA.

Correspondence: Ray E. Hershberger (rhershberger@med.miami.edu)

DOI: 10.1111/j.1752-8062.2010.00249.x

### Mutagenesis and Heterologous Expression

SCN5A mutations R222Q and I1835T were created by site-directed mutagenesis using a mutagenesis kit (Stratagene, La Jolla, CA, USA) and were engineered both separately and together with H558R on the same cDNA construct into two common splice variants of human cardiac voltage-dependent sodium channel SCN5A (one lacking a glutamine at position 1077 is noted as Q1077del [Genbank accession no. AY148488], another containing Q1077 is noted as Q1077 [Genbank accession no. AC1377587]) in the pcDNA3 plasmid vector (Invitrogen, Carlsbad, CA, USA) as previously reported.<sup>13–15</sup> All clones were sequenced to confirm integrity and to ensure the presence of the introduced mutations and the absence of other substitutions caused by PCR. The wild type (WT) and mutant channels were transiently transfected into HEK293 cells

with FuGENE6 reagent (Roche Diagnostics, Indianapolis, IN, USA) according to the manufacturer's instructions.

### Electrophysiological measurements

Macroscopic voltage-gated  $I_{Na}$  was measured 24 hours after transfection with the standard whole-cell patch clamp method at 21°C–23°C in the HEK293 cells. Microelectrodes were manufactured from borosilicate glass using a puller (P-87, Sutter Instrument Co, Novato, CA, USA) and were heat polished with a microforge (MF-83, Narishige, Tokyo, Japan). The resistances of microelectrodes ranged from 1.0 to 2.0 MΩ. Voltage clamp data were generated with pClampex 10.2 and analyzed using Clampfit 10.2 (Molecular Devices Corporation, Sunnyvale, CA, USA). Membrane current data were digitalized at 100 kHz, low-pass filtered at 5 kHz, and then normalized to membrane capacitance. The extracellular and intracellular solution formulas and the standard voltage clamp protocols are presented in supplemental materials, as described in detail previously.<sup>13–15,19</sup>

### Statistical Analysis

All data points are reported as the mean value and the standard error of the mean (SEM). Determinations of statistical significance were performed using a Student's *t*-test for comparisons of two means or using analysis of variance (ANOVA) for comparisons of multiple groups. Statistical significance was determined by a value of  $p < 0.05$ .

### Results

#### Clinical phenotypes and genetic analysis

Two missense SCN5A rare protein altering variants were identified in two probands with familial DCM, as previously reported.<sup>12</sup> Probands and affected family members had DCM with prominent CSD, as previously noted in prior SCN5A DCM reports.<sup>2–6</sup> We show here that both segregated with DCM in multiple affected family members (Figure 1, Table 1). Both probands were negative for

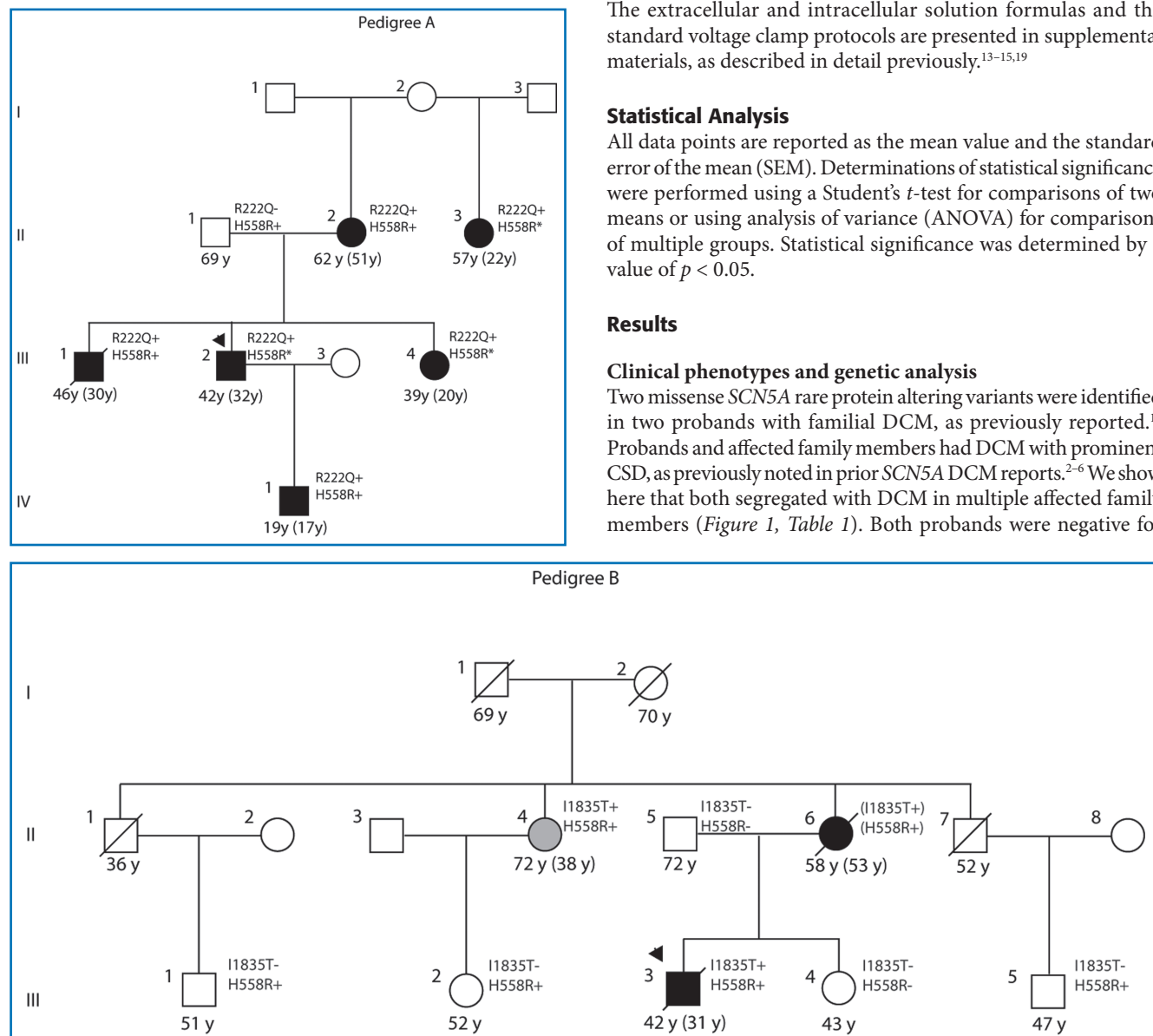


**Figure 1.** Pedigrees of SCN5A related cardiomyopathy. Pedigrees have been labeled by letter (A) and (B), which correspond to their respective mutation as shown in Table 1. Squares represent males, circles females. An arrowhead denotes the proband. A diagonal line marks deceased individuals. Solid symbols indicate idiopathic dilated cardiomyopathy (IDC) with or without heart failure; shaded symbols represent any cardiovascular abnormality. Open symbols represent unaffected individuals. For IDC cases, current age or age at death and age at IDC diagnosis or cardiovascular abnormality finding (in parenthesis) is presented. The presence or absence of the pedigree's SCN5A mutation is indicated by a + or – symbol, respectively, next to the identified variant (R222Q or I1835T). Obligate carriers are noted in parenthesis, (+). Genotype for the H558R polymorphism is denoted H558R+ (present) or H558R– (absent) or H558R\* (homozygous).

Pedigree member	Age (years)	DCM	ECG/Arrhythmia	QTc (ms)	Heart rate	LVEDD, mm (Z-score)	LV septum, posterior wall thickness, mm	EF	SCN5A mutation	H558R polymorphism	Comment
<b>Pedigree A: R222Q</b>											
III-2	32	Yes	Bigem	NA	NA	74 (5.6)	11, 11	18%	R222Q	Yes, homozygous	Proband, HF, ICD
II-1	NA	No	NA	NA	NA	NA	NA	NA	No	Yes	
II-2	51	Yes	LAE, PACs, PVCs	NA	NA	57 (3.7)	NA	30%	R222Q	Yes	HF, AF
II-3	22	Yes	1AVB, AF, LBBB, LVH, NSST	439, 455	112, 95	60 (4.3)	NA	28%	R222Q	Yes	PPCM
III-1	30	Yes	LBBB	NA	NA	84 (7.1)	7,7	15%	R222Q	Homozygous Yes	HF, ICD, PM
III-4	20	Yes	NA	NA	NA	70 (6.6)	7,8	15%	R222Q	Yes, homozygous	HF, ICD
IV-1	17	Yes	Multifocal PVCs, bigem	385	96	78 (6.3)	8,9	13%	R222Q	Yes	
<b>Pedigree B: I1835T</b>											
III-3	31	Yes	NSCD, LAE, PVC, borderline IVCD, 1AVB, NSST	465	78	84 (7.0)	11,9	10%	I1835T	Yes	Proband, HF, ICD, PM, sudden death
II-4	NA	No	AF, 1AVB, PAC	402	59	56 (2.6)	12,12	65%	I1835T	Yes	LVE, tachyarrhythmia
II-6	53	Yes	unifocal PVCs, LAD, NSST	NA	NA	71 (6.5)	7,9	NA	I1835T	Yes	FS = 25%, HF, paroxysmal hypertension
III-1	NA	No	No	385	63	53 (-0.2)	10,10	60%	No	Yes	
III-2	NA	No	No	402	53	45 (-0.7)	9,9	73%	No	Yes	
III-4	NA	No	No	399	52	49 (0.9)	9,11	70%	No	No	
III-5	NA	No	Borderline LVH	332	NA	61 (2.5)	10,9	59%	No	Yes	LVE

Age indicates age of diagnosis; 1AVB = first-degree atrioventricular block; AF = atrial fibrillation; bigem = bigeminy; DCM = dilated cardiomyopathy; EF = ejection fraction; FS = fractional shortening; HF = heart failure; ICD = implantable cardiac defibrillator; int = intermittent; IVCD = intraventricular conduction delay; LAD = left axis deviation; LAE = left atrial enlargement; LBBB = left bundle branch block; LVE = left ventricular enlargement; LVEDD = left ventricular end-diastolic dimension; LVH = left ventricular hypertrophy; NA = not available; NSCD = nonspecific conduction delay; NSST = nonspecific ST-T changes; PAC = premature atrial contractions; PM = pacemaker; PPCM = peripartum cardiomyopathy; PVC = premature ventricular contractions; VT = ventricular tachycardia.

**Table 1.** Clinical characteristics of individuals in pedigrees A and B with DCM.

rare variants from 14 other DCM genes (*PSEN1*, *PSEN2*, *LMNA*, *MYH7*, *TNNT2*, *LDB3*, *TCAP*, *MLP*, *MYBPC3*, *MYH6*, *TPM1*, *TNNC1*, *TNNI3*, and *RBM20*), as previously published.<sup>12,17,18,20,21</sup>

In Pedigree A, the variant R222Q (a G > A substitution in codon 222 causing the substitution of arginine by glutamine) segregated with IDC and was therefore considered likely disease causing.<sup>12</sup> DCM in this non-Hispanic white family was characterized by early onset disease (approximately 29 years of age) and prominent CSD. The proband (III-2) and his siblings (III-1 and III-4) required an implantable cardiac defibrillator (ICD) at ages 32, 31, and 23, respectively. The proband's son (IV-1) had asymptomatic premature ventricular contractions (PVCs) detected at age 10 during screening, preceding a DCM diagnosis at age 17. Notably, all of the six affected R222Q carriers were either homozygous with the *SCN5A* common polymorphism H558R or heterozygous with the H558R on the same allele (Table 1, Figure 1A).

In Pedigree B, the mutation I1835T (a T > C substitution in code 1835, resulting in the substitution of isoleucine by

threonine), classified as likely disease causing, segregated with DCM in an African-American family and was not observed in 422 DNAs (844 chromosomes) of which 193 DNAs were African American.<sup>12</sup> The two affected I1835T carriers were heterozygous with H558R on the same allele. The proband (III-3) was diagnosed with DCM at age 31 after a screening echocardiogram revealed left ventricular enlargement and a low normal EF. He was asymptomatic at the time, but 6 years later, heart failure symptoms began, his left ventricular end-diastolic size was found to be increased by 15 mm and his EF had decreased to 10%. Medical treatment was initiated. An ICD was placed a year later. He died suddenly at the age of 42. His mother (II-6), who also had a history of CSD, was diagnosed with DCM at age 53, and died 5 years later. Her death certificate stated the cause of death as sudden cardiac death and arrhythmia. Subject III-5, who was found not to carry the I1835T variant, had left ventricular enlargement with preserved systolic function, possibly due to environmental or other genetic factors.

Samples	Peak $I_{Na}$		Activation			Inactivation			Late $I_{Na}$	
	pA/pF	n	$V_{1/2}$ (mV)	K	n	$V_{1/2}$ (mV)	K	n	%	n
in Q1077del background										
WT	-286 ± 37	15	-32.2 ± 0.8	4.6 ± 0.3	16	-79.7 ± 0.9	5.0 ± 0.1	17	0.16 ± 0.06	12
H558R	-311 ± 46	13	-32.5 ± 1.1	4.9 ± 0.3	13	-79.1 ± 0.7	5.1 ± 0.1	13	0.07 ± 0.03	11
R222Q	-240 ± 31	14	-45.3 ± 0.6†	5.2 ± 0.2	13	-83.9 ± 0.8†	4.5 ± 0.2	13	0.08 ± 0.03	10
R222Q/H558R	-184 ± 17*	19	-43.6 ± 0.6†	5.6 ± 0.3‡	18	-84.5 ± 0.5†	4.8 ± 0.1	19	0.05 ± 0.02	12
in Q1077 background										
WT	-232 ± 42	8	-31.1 ± 1.4	3.8 ± 0.3	6	-70.6 ± 1.1	4.6 ± 0.2	8	0.16 ± 0.08	6
H558R	-302 ± 43	6	-32.0 ± 0.9	4.3 ± 0.3	7	-71.6 ± 0.8	5.1 ± 0.4	7	0.08 ± 0.06	7
R222Q	-277 ± 63	7	-46.5 ± 2.6†	4.7 ± 0.5	6	-78.6 ± 1.3†	4.1 ± 0.2	9	0.13 ± 0.04	8
R222Q/H558R	-239 ± 69	8	-41.7 ± 1.3†	4.6 ± 0.3	8	-74.5 ± 0.6*	4.2 ± 0.2	8	0.14 ± 0.07	6

$I_{Na}$  = sodium current; pA/pF = current density;  $V_{1/2}$  = voltage of half-maximal activation/inactivation; K = slope factor. Values are mean ± SE for n experiments. All parameters were analyzed using one-way ANOVA followed by a Tukey test. Compared to corresponding WT, \* =  $p < 0.01$ ; † =  $p < 0.001$ ; ‡ =  $p < 0.05$ .

**Table 2.** Biophysical properties of WT or R222Q associated variant sodium channels in HEK293 cells.

### Biophysical phenotype of R222Q-related channels

We first studied WT, H558R, R222Q, and R222Q/H558R (two variants on the same construct) using the Q1077del background, the more abundant alternatively spliced SCN5A transcript (approximately 65%) in human hearts.<sup>13</sup>  $I_{Na}$  densities of WT, H558R, and R222Q by themselves showed no significant differences, but R222Q/H558R caused a approximately 35% reduction (Table 2). The voltage  $I_{Na}$  density relationship indicated R222Q/H558R decreased  $I_{Na}$  densities through various test potentials compared to WT (Figure 2A). Compared with WT, no variants altered late  $I_{Na}$  (Table 2).

The R222Q mutation was located in the voltage sensor of  $N_{aV}1.5$ , and not unexpectedly caused drastic alterations in both voltage dependence of steady-state activation and inactivation. Compared with WT, the activation and inactivation curves for R222Q exhibited a negative shift by -13 mV and -4 mV, respectively. R222Q/H558R showed similar changes in both activation and inactivation parameters to R222Q (Table 2; Figure 2B and C). The parallel shift in both activation and inactivation did not change the window current for R222Q and R222Q/H558R compared with WT (Figure 2D). Moreover, only R222Q/H558R showed slower recovery from inactivation and had increased time constants ( $\tau_p$ , 2.20 ± 0.19 ms;  $\tau_s$ , 84.4 ± 7.1 ms;  $n = 17$ ;  $p < 0.01$ ) values compared with WT ( $\tau_p$ , 1.55 ± 0.13 ms;  $\tau_s$ , 38.3 ± 3.5 ms;  $n = 16$ ) (Figure 2E). We analyzed the decay phase of macroscopic  $I_{Na}$  across several test potentials using a two-exponential fit. Compared with WT, there was no difference in both time constants ( $\tau_f$ ,  $\tau_s$ ) and fractional amplitudes of two components observed in these variants (data not shown).

To determine if the less abundant alternatively spliced transcript exerted an effect on these variants, we also tested the WT, H558R, R222Q, and R222Q/H558R in the Q1077 background. In contrast to Q1077del, all variants in Q1077 showed comparable peak  $I_{Na}$  densities to WT (Table 2). The late  $I_{Na}$  also showed no difference between each group (Table 2). Nevertheless, both R222Q and R222Q/H558R exhibited a significant negative shift in both activation and inactivation and those alterations did not affect the window current in Q1077 background (data not shown). Both the recovery from inactivation and decay of the peak  $I_{Na}$  for all variants showed no difference compared to WT (data not shown).

### Biophysical phenotype for I1835T-associated channels

In the Q1077del background, H558R and I1835T exhibited no differences but I1835T/H558R (on the same construct) showed approximate 30% decrease in the peak  $I_{Na}$  densities (Table 3) compared with WT. The relationships between voltage and  $I_{Na}$  density indicated I1835T/H558R attenuated  $I_{Na}$  densities through multiple test potentials compared to WT (Figure 3A). All variants showed comparable late  $I_{Na}$  to WT (Table 3).

For voltage dependence of steady-state activation, all variants showed no differences from WT (Figure 3B). In steady-state inactivation curves, only I1835T/H558R caused a negative shift by -3.6 mV compared to WT ( $p < 0.01$ ) (Figure 3C). Thus, the window current for I1835T/H558R tended to decrease compared with WT (Figure 3D). The reduction of window current may decrease the channel availability to contribute to the attenuation in peak  $I_{Na}$ . As for recovery from inactivation, only I1835T/H558R showed slower recovery from inactivation and had significantly increased time constants ( $\tau_p$ , 2.40 ± 0.22 ms;  $\tau_s$ , 50.2 ± 6.0 ms;  $n = 12$ ;  $p < 0.01$ ) values than WT ( $\tau_p$ , 1.43 ± 0.09 ms;  $\tau_s$ , 33.1 ± 3.9 ms;  $n = 11$ ) (Figure 3E) at 0 mV. Compared with WT, only I1835T/H558R showed slower current decay and had larger fast component time constant values across several test potentials (Figure 3F). There was no difference in both time constants ( $\tau_p$ ,  $\tau_s$ ) and fractional amplitudes of two components observed in other mutants (data not shown).

In the Q1077 background, the peak  $I_{Na}$  densities for all variants showed no differences from WT and all these variants did not affect the late  $I_{Na}$  significantly compared to WT (Table 3). There was no difference between WT and all variants in steady-state activation (Table 3), and only I1835T/H558R still showed a negative shift by -4.3 mV in steady-state inactivation (Table 3) and tended to decrease the window current compared with WT ( $p < 0.05$ ) (data not shown). However, no differences were found in both recovery from inactivation and current decay between all groups (data not shown).

### Discussion

The principal finding of this study is that common variants in SCN5A play an essential role in the cellular biophysical phenotype for the two novel DCM-related SCN5A rare variants, R222Q and I1835T. While prior reports<sup>2-6</sup> like ours<sup>12</sup> have shown that



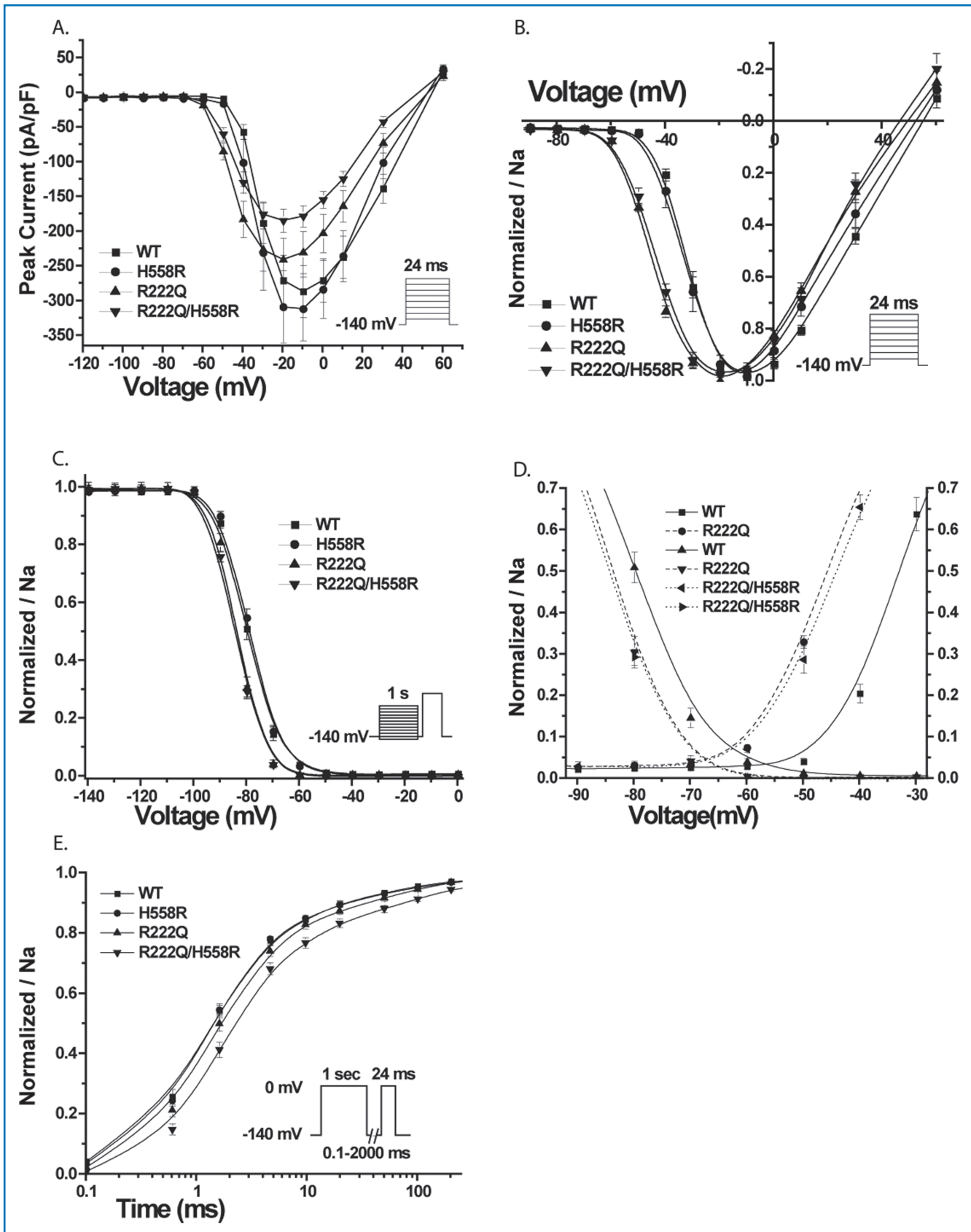


**Figure 2.** Biophysical properties of R222Q-SCN5A associated mutations in the Q1077del background. Standard patch clamp protocols are depicted in the inset of each figure. (A) Peak current-voltage relationships. (B) Voltage dependence of activation for WT and variants. (C) Steady-state inactivation for WT and variants. (D) The peak current activation data are replotted as a conductance ( $G$ ) curve with steady-state inactivation relationships to show the overlap of these relationships (window current). (E) Time course of recovery from inactivation was elicited using the protocol described in the inset. R222Q/H558R exhibited slower recovery from inactivation than WT (time is on a log scale).

Samples	Peak $I_{Na}$		Activation		Inactivation			Late $I_{Na}$		
	pA/pF	n	$V_{1/2}$ (mV)	K	n	$V_{1/2}$ (mV)	K	n	%	n
in Q1077del background										
WT	$-320 \pm 51$	11	$-34.9 \pm 1.2$	$4.1 \pm 0.2$	9	$-72.0 \pm 0.8$	$4.6 \pm 0.2$	11	$0.16 \pm 0.08$	11
H558R	$-333 \pm 54$	6	$-34.1 \pm 1.2$	$4.0 \pm 0.3$	5	$-71.9 \pm 0.9$	$4.7 \pm 0.5$	6	$0.18 \pm 0.09$	6
I1835T	$-262 \pm 70$	7	$-34.5 \pm 1.1$	$3.8 \pm 0.3$	5	$-70.3 \pm 1.0$	$4.4 \pm 0.2$	7	$0.19 \pm 0.07$	5
I1835T/H558R	$-218 \pm 45^*$	14	$-33.9 \pm 0.9$	$4.3 \pm 0.2$	10	$-75.6 \pm 0.7^\dagger$	$5.6 \pm 0.2^*$	13	$0.16 \pm 0.06$	12
in Q1077 background										
WT	$-269 \pm 44$	7	$-34.9 \pm 0.9$	$3.7 \pm 0.3$	5	$-72.9 \pm 1.0$	$5.3 \pm 0.3$	7	$0.09 \pm 0.06$	5
H558R	$-249 \pm 69$	5	$-35.0 \pm 0.7$	$3.5 \pm 0.2$	5	$-71.8 \pm 2.5$	$4.3 \pm 0.4$	5	$0.09 \pm 0.06$	5
I1835T	$-253 \pm 41$	8	$-34.4 \pm 1.5$	$3.9 \pm 0.2$	8	$-72.4 \pm 1.0$	$5.0 \pm 0.2$	8	$0.08 \pm 0.04$	9
I1835T/H558R	$-288 \pm 53$	8	$-34.3 \pm 1.8$	$4.3 \pm 0.4$	6	$-77.2 \pm 1.0^*$	$5.4 \pm 0.3$	8	$0.10 \pm 0.04$	7

All parameters were analyzed using one-way ANOVA followed by a Tukey test. \* =  $p < 0.05$  versus WT; † =  $p < 0.01$  versus WT.

**Table 3.** Biophysical properties of WT or I1835T associated variant sodium channels in HEK293 cells.

SCN5A rare variants are associated with DCM, we now show that DCM-related SCN5A mutations, R222Q and I1835T, caused 35% and 30% decreases, respectively, in peak  $I_{Na}$  density, which were dependent upon the common polymorphism H558R and the alternative splice variant Q1077del background.

Collectively, these biophysical findings, combined with the clinical, pedigree, and molecular genetic data provide additional evidence that these two SCN5A rare variants are associated with CSD and DCM. Each mutation segregated with DCM and CSD in multiple affected members in both families, even though one mutation carrier in Pedigree B (II-4) had less penetrant disease as has been commonly observed in genetic DCM. These variants were absent in unaffected family members and were not identified in control DNAs.<sup>12</sup> No other rare variants were identified in 14 other DCM-susceptibility genes in DNA specimens of each family's proband.<sup>12,17,18,20,21</sup>

The clinical characteristics of patients with DCM, attributed to rare variants in >30 genes, are diverse and vary considerably, even in patients or families harboring the same mutation.<sup>1</sup> These DCM characteristics include age of onset, the severity and rate of progression, whether prominent CSD precedes, accompanies, or follows the DCM, whether heart failure or arrhythmia occurs, and other features.<sup>1</sup> We suggest that a principal inference from this study is that other yet undefined genetic backgrounds, as shown here for these SCN5A mutations, may also modulate the cellular and clinical DCM phenotypes arising from many different rare variant causes. Although this concept is plausible, it has been particularly challenging to identify specific factors, whether environmental or genetic, which influence the DCM or CSD phenotypes. While the biophysical evidence presented here is compelling, other relevant genetic backgrounds may also affect SCN5A (or other DCM gene) function, even though gaining clinical insight by correlating the effects of polymorphisms on rare variants from family-based clinical data is difficult even with large families, as in most cases the family members who carry a rare variant will also carry the same common variant, as illustrated by these two families.

The SCN5A splice variants, Q1077del and Q1077, exist in the human heart at an mRNA ratio of approximately 2:1, and were shown to affect the SCN5A biophysical phenotype in our prior studies<sup>13,15</sup> as well as this study. However, to our

knowledge, all known DCM-associated SCN5A mutations have been characterized in only the Q1077 background. The Q1077del or Q1077 background has also been shown to be relevant for SCN5A rare variants identified in phenotypes other than DCM. The plasma membrane protein expression levels of the Brugada syndrome (BrS) G1406R mutation was influenced by the Q1077del/Q1077 background.<sup>22</sup> Also, depending on Q1077del background, cotransfection of H558R with Y389X decreased  $I_{Na}$  densities significantly.<sup>23</sup> Further, the SCN5A mutations delAL586-587, R680H, V1951L,<sup>24</sup> and R680H/S1103Y<sup>25</sup> required the Q1077del background to exhibit late  $I_{Na}$ . These studies suggest, as do ours, that the Q1077del/Q1077 background may be a splice variant-based regulatory mechanism for normal function in the cardiac sodium channel analogous to other voltage-gated cardiac ion channels regulated by subunit splice variants, such as the potassium channel  $K_v11.1$ ,<sup>26</sup> the L-type calcium channel  $Ca_v1.2$ ,<sup>27</sup> the type 2 ryanodine receptor (RyR2),<sup>28</sup> and the calcium channel  $\beta_2$  subunit.<sup>29</sup>

As the major pathway for sodium influx in the cardiac myocyte, the sodium channel is responsible for adjusting the intracellular sodium concentration.<sup>30</sup> As shown here, in SCN5A-related DCM, the reduced  $I_{Na}$  may interfere with intracellular sodium homeostasis, disrupting  $Na^+/Ca^{2+}$  and  $Na^+/H^+$  exchange, thereby changing the intracellular pH and  $Ca^{2+}$  homeostasis to disturb the excitation-contraction coupling and energy production mechanisms.<sup>31</sup> However, whether these cellular electrophysiological variations from WT identified in heterologous cell systems are directly linked to the development of the DCM phenotype (i.e., progressive myocardial dysfunction as distinctive from CSD) remains enigmatic.

While other DCM-associated SCN5A rare variants have shown qualitatively similar biophysical findings as those reported here, they have varied considerably quantitatively from one another and have not correlated with DCM severity. Specifically, of the nine previously characterized DCM-related SCN5A mutations, five variants (W156X, R225W, T220I, R814Q, and D1595N)<sup>2,8-10</sup> showed mild decrease to complete abolition in peak  $I_{Na}$  density, raising doubt of this specific mechanism itself leading to DCM. Hence, the possibility that additional genetic background may influence the DCM phenotype is likely. Rare variants may be present in many other, yet undiscovered genes, that are relevant

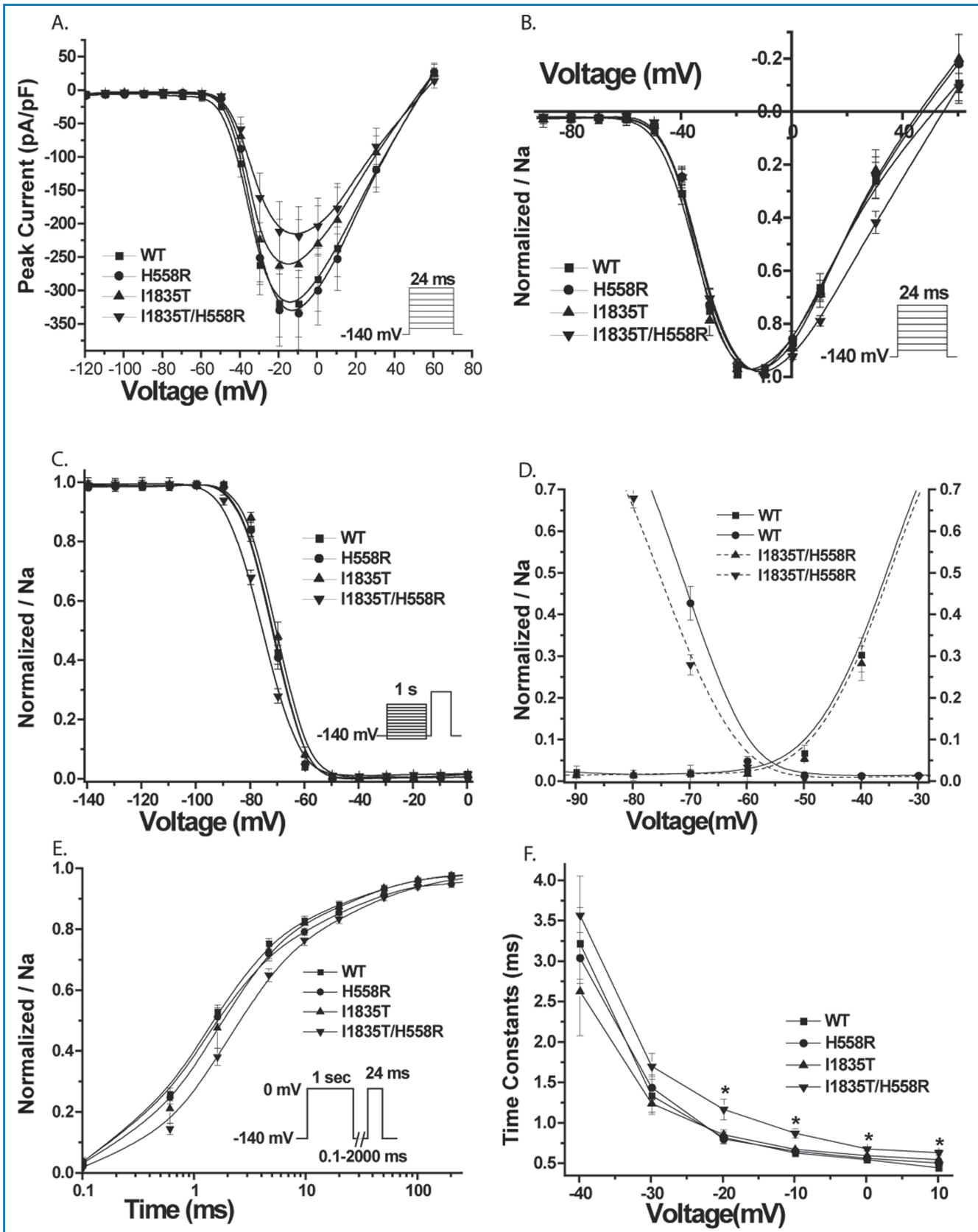


**Figure 3.** Biophysical properties of I1835T-SCN5A associated mutations in the Q1077del background. (A) Peak current-voltage relationships. (B) Voltage dependence of activation for WT and variants. (C) Steady-state inactivation for WT and variants. (D) The peak current activation data are replotted as a conductance (G) curve with steady-state inactivation relationships to show the overlap of these relationships (window current). (E) I1835T/H558R exhibited slower recovery from inactivation than WT (time is on a log scale). (F) Decay of macroscopic current. Compared with WT, I1835T/H558R showed significantly larger fast component ( $\tau_f$ ) values across a wide range of test potentials from  $-20$  mV to  $10$  mV. \* $p < 0.05$  versus WT.

for DCM,<sup>32</sup> as only approximately 35% of DCM genetic cause has been identified,<sup>1,20</sup> and DCM shows marked locus and allelic heterogeneity.<sup>1,32</sup>

### Limitations

The biophysical phenotypes of these *SCN5A* rare variants were obtained in heterologous systems that may not faithfully recapitulate the phenotypes found in cardiac myocytes. However, inducing cardiomyocytes from pluripotent stem cells derived from individual patients holds the promise for the study of  $I_{Na}$ -associated DCM in the relevant genetic and human background.<sup>33</sup> Although nonsynonymous rare variants in 14 other DCM genes were excluded, other unknown and undetected common or rare variants may have affected the *SCN5A* rare variant DCM phenotype. Further, only coding sequence was examined. However, we estimate that rare variants in these 14 genes represent approximately three-quarters of known rare variant genetic cause, and to date almost all mutations implicated to cause DCM arise in coding or splice site sequence.

### Conclusion

In conclusion, the impact of the common polymorphisms H558R and Q1077del on the *SCN5A* rare variant biophysical phenotypes illustrates the key role of genetic background on *SCN5A* rare variants, and by inference, the potential role of genetic background for other rare variants that cause DCM.

### Acknowledgments

We thank the families for their participation in the Familial Dilated Cardiomyopathy Research Program, without whom these studies would not have been possible.

### Sources of Funding

Funding was provided by the University of Wisconsin Cellular and Molecular Arrhythmia Research Program (to J.C.M.), grants HL58626 (to R.E.H.), HL71092 (to J.C.M.) from National Institutes of Health, USA, and the grant 30973367 (to J.C.) from the National Natural Science Foundation of China.

### Disclosures

None.

### References

- Hershberger RE, Cowan J, Morales A, Siegfried JD. Progress with genetic cardiomyopathies: screening, counseling, and testing in dilated, hypertrophic, and arrhythmogenic right ventricular dysplasia/cardiomyopathy. *Circ Heart Fail*. 2009; 2:253–261.
- Bezzina CR, Rook MB, Groenewegen WA, Herfst LJ, Van Der Wal AC, Lam J, et al. Compound heterozygosity for mutations (W156X and R225W) in *SCN5A* associated with severe cardiac conduction disturbances and degenerative changes in the conduction system. *Circ Res*. 2003; 92:159–168.
- McNair WP, Ku L, Taylor MR, Fain PR, Dao D, Wolfel E, et al. *SCN5A* mutation associated with dilated cardiomyopathy, conduction disorder, and arrhythmia. *Circulation*. 2004; 110:2163–2167.
- Olson TM, Michels VV, Ballew JD, Reyna SP, Karst ML, Herron KJ, et al. Sodium channel mutations and susceptibility to heart failure and atrial fibrillation. *JAMA*. 2005; 293:447–454.
- Ge J, Sun A, Paajanen V, Wang S, Su C, Yang Z, et al. Molecular and clinical characterization of a novel *SCN5A* mutation associated with atrioventricular block and dilated cardiomyopathy. *Circ Arrhythm Electrophysiol*. 2008; 1:83–92.
- Nguyen TP, Wang DW, Rhodes TH, George AL, Jr. Divergent biophysical defects caused by mutant sodium channels in dilated cardiomyopathy with arrhythmia. *Circ Res*. 2008; 102:364–371.
- Bezzina CR, Remme CA. Dilated cardiomyopathy due to sodium channel dysfunction: what is the connection? *Circ Arrhythm Electrophysiol*. 2008; 1:80–82.

- Benson DW, Wang DW, Dymont M, Knilans TK, Fish FA, Strieper MJ, et al. Congenital sick sinus syndrome caused by recessive mutations in the cardiac sodium channel gene (*SCN5A*). *J Clin Invest*. 2003; 112:1019–1028.
- Chen LQ, Santarelli V, Horn R, Kallen RG. A unique role for the S4 segment of domain 4 in the inactivation of sodium channels. *J Gen Physiol*. 1996; 108:549–556.
- Wang DW, Viswanathan PC, Balsler JR, George AL, Jr, Benson DW. Clinical, genetic, and biophysical characterization of *SCN5A* mutations associated with atrioventricular conduction block. *Circulation*. 2002; 105:341–346.
- Groenewegen WA, Firouzi M, Bezzina CR, Vliex S, van Langen IM, Sandkuijl L, et al. A cardiac sodium channel mutation cosegregates with a rare connexin40 genotype in familial atrial standstill. *Circ Res*. 2003; 92:14–22.
- Hershberger RE, Parks SB, Kushner JD, Li D, Ludwigsen S, Jakobs P, et al. Coding sequence mutations identified in MYH7, TNNT2, *SCN5A*, *CSR3P3*, *LBD3*, and *TCAP* from 313 patients with familial or idiopathic dilated cardiomyopathy. *Clin Transl Sci*. 2008; 1:21–26.
- Makielski JC, Ye B, Valdivia CR, Pagel MD, Pu J, Tester DJ, et al. A ubiquitous splice variant and a common polymorphism affect heterologous expression of recombinant human *SCN5A* heart sodium channels. *Circ Res*. 2003; 93:821–828.
- Ye B, Valdivia CR, Ackerman MJ, Makielski JC. A common human *SCN5A* polymorphism modifies expression of an arrhythmia causing mutation. *Physiol Genomics*. 2003; 12:187–193.
- Tan BH, Valdivia CR, Rok BA, Ye B, Ruwaldt KM, Tester DJ, et al. Common human *SCN5A* polymorphisms have altered electrophysiology when expressed in Q1077 splice variants. *Heart Rhythm*. 2005; 2:741–747.
- Kushner JD, Nauman D, Burgess D, Ludwigsen S, Parks S, Pantely G, et al. Clinical characteristics of 304 kindreds evaluated for familial dilated cardiomyopathy. *J Card Fail*. 2006; 12:422–429.
- Li D, Parks SB, Kushner JD, Nauman D, Burgess D, Ludwigsen S, et al. Mutations of presenilin genes in dilated cardiomyopathy and heart failure. *Am J Hum Genet*. 2006; 79:1030–1039.
- Parks SB, Kushner JD, Nauman D, Burgess D, Ludwigsen S, Peterson A, et al. Lamin A/C mutation analysis in a cohort of 324 unrelated patients with idiopathic or familial dilated cardiomyopathy. *Am Heart J*. 2008; 156:161–169.
- Cheng J, Van Norstrand DW, Medeiros-Domingo A, Valdivia C, Tan BH, Ye B, et al. Alpha 1-syntrophin mutations identified in sudden infant death syndrome cause an increase in late cardiac sodium current. *Circ Arrhythm Electrophysiol*. 2009; 2:667–676.
- Hershberger R, Norton N, Morales A, Li D, Siegfried J, Gonzalez-Quintana J. Coding sequence rare variants identified in MYBPC3, MYH6, TPM1, TNNC1 And TNNT3 from 312 patients with familial or idiopathic dilated cardiomyopathy. *Circ Cardiovasc Genet*. 2010; 3:155–161.
- Li D, Morales A, Gonzalez Quintana J, Norton N, Siegfried JD, Hofmeyer M, et al. Identification of novel mutations in *RBM20* in patients with dilated cardiomyopathy. *Clin Transl Sci*. 2010; 3:90–97.
- Tan BH, Valdivia CR, Song C, Makielski JC. Partial expression defect for the *SCN5A* missense mutation G1406R depends on splice variant background Q1077 and rescue by mexiletine. *Am J Physiol Heart Circ Physiol*. 2006; 291:H1822–H1828.
- Maginot KR, Haas N, January CT, Makielski JC, Valdivia CR. A common polymorphism may dramatically affect phenotype in a family with a novel nonsense *SCN5A* mutation. *Heart Rhythm*. 2009; 6:S198(abstract).
- Wang DW, Desai RR, Crotti L, Arnestad M, Insolia R, Pedrazzini M, et al. Cardiac sodium channel dysfunction in sudden infant death syndrome. *Circulation*. 2007; 115:368–376.
- Cheng J, Tester DJ, Tan BH, Valdivia C, Kroboth S, Ye B, et al. The *SCN5A* mutation R680H from sudden death interacts with a polymorphism *SCN5A*-S1103Y common in African Americans to increase late sodium current. *Circulation*. 2009; 120:S662(abstract).
- Wang X, Xu R, Abernathy G, Taylor J, Alzghoul MB, Hannon K, et al. Kv11.1 channel subunit composition includes MinK and varies developmentally in mouse cardiac muscle. *Dev Dyn*. 2008; 237:2430–2437.
- Liao P, Yu D, Li G, Yong TF, Soon JL, Chua YL, et al. A smooth muscle Cav1.2 calcium channel splice variant underlies hyperpolarized window current and enhanced state-dependent inhibition by nifedipine. *J Biol Chem*. 2007; 282:35133–35142.
- George CH, Rogers SA, Bertrand BM, Tunwell RE, Thomas NL, Steele DS, et al. Alternative splicing of ryanodine receptors modulates cardiomyocyte Ca<sup>2+</sup> signaling and susceptibility to apoptosis. *Circ Res*. 2007; 100:874–883.
- Chu PJ, Larsen JK, Chen CC, Best PM. Distribution and relative expression levels of calcium channel beta subunits within the chambers of the rat heart. *J Mol Cell Cardiol*. 2004; 36:423–434.
- Bers DM, Barry WH, Despa S. Intracellular Na<sup>+</sup> regulation in cardiac myocytes. *Cardiovasc Res*. 2003; 57:897–912.
- Frustraci A, Priori SG, Pileri M, Chimenti C, Napolitano C, Rivolta I, et al. Cardiac histological substrate in patients with clinical phenotype of Brugada syndrome. *Circulation*. 2005; 112:3680–3687.
- Hershberger RE. A glimpse into multigene rare variant genetics: triple mutations in hypertrophic cardiomyopathy. *J Am Coll Cardiol*. 2010; 55:1454–1455.
- Kamp TJ, Lyons GE. On the road to iPSC cell cardiovascular applications. *Circ Res*. 2009; 105:617–619.